

## BOND PROPERTIES OF MICRO-FIBERS IN CEMENTITIOUS MATRIX

Amnon Katz<sup>1</sup> and Victor C. Li

Advanced Civil Engineering Materials Research Laboratory

Department of Civil and Environmental Engineering

University of Michigan, MI 48105-2125, U.S.A.

### ABSTRACT

Using a new technique for pullout test of microfibers, the interfacial bond properties of two carbon fibers having a diameter of 10  $\mu\text{m}$  and 46  $\mu\text{m}$  were tested and compared with those of high modulus polyethylene and steel fibers having a diameter of 42  $\mu\text{m}$  and 18  $\mu\text{m}$ , respectively. The fibers were embedded in cement matrices of different water to binder ratio and silica-fume content.

By studying the complete pullout load-pullout displacement curve and by using Environmental Scanning Electron Microscope (ESEM), it was found that the bond mechanism is mainly of friction for the fine and smooth carbon and polyethylene fibers. For the large carbon fiber and steel fiber, mechanical anchorage is the main bond mechanism.

### INTRODUCTION

Interfacial fiber-matrix properties serve as an important parameter with the use of fibers in composite materials. Most composite models are based on the pullout behavior of a single fiber, assuming a constant frictional bond between the fiber and the matrix, independent of slip. P-u (pullout load vs. displacement) relationship was developed by Li [1], assuming constant friction (Fig. 1).

The pre-peak P-u relationship typically shows a non-linear behavior due to the debonding process and fiber stretching with increasing load, while the post-peak relationship shows a linear decrease as the embedded length of the fiber becomes shorter when the fiber is pulled out (line a in Fig. 1).

However, studies done by Wang et al. [2] on Nylon fibers and Naaman et al. [3] on steel fibers showed slip-hardening or slip-weakening behavior, respectively, as the fiber-matrix interaction is changed due to damage of the interface, associated with the relative stiffness of fiber and matrix. For stiff matrix and relatively weak fiber it might be slip-hardening behavior (line c in Fig. 1), due to peeling of the fiber by the stiff matrix (Wang et al. [2]). For a stiff fiber and a relatively weak matrix it might be slip-weakening behavior (line b in Fig. 1), due to rapid destruction of the matrix around the fiber as it is pulled out (Naaman et al. [3]).

---

<sup>1</sup>Present address: National Building Research Institute, Technion - Israel Institute of Technology, Haifa 32000, Israel.

In this work, the bond properties of micro-fibers were studied by using the direct pullout technique developed by Katz and Li [4] and by using an Environmental Scanning Electron Microscope (ESEM) for different matrix compositions and micro-fiber types, in order to determine the pullout behavior of this kind of fibers for different matrices.

## EXPERIMENTAL

Four micro-fiber types were tested in the experimental program: Fiber A - high modulus polyethylene fiber ('Spectra 900') having a diameter of  $d=42\text{ }\mu\text{m}$  and modulus of elasticity of  $E_f=120\text{ GPa}$ ; Fiber B - steel fiber,  $d=18\text{ }\mu\text{m}$  and  $E_f=210\text{ GPa}$ ; Fiber C - carbon fiber,  $d=10\text{ }\mu\text{m}$  and  $E_f=240\text{ GPa}$ ; and Fiber D - carbon fiber,  $d=46\text{ }\mu\text{m}$  and  $E_f=175\text{ GPa}$ . Two water to binder (cementitious materials) ratios were tested: low ( $w/b=0.35$ ) and high ( $w/b=0.50$ ). The effect of silica-fume, which improves the density of the matrix and possibly also the interface, was also studied in the experimental program. The composition of the different mixes is listed in Table 1. All fiber types were tested for all the matrices in Table 1 at the age of 14 days.

### Test procedure

Direct pullout testing of a fine brittle fiber, such as carbon fiber, from a cementitious matrix, is difficult to carry out as fiber orientation is changed due to local bending while casting or the fiber breaks during the pullout test due to local bending of the fiber close to the matrix or the gripper of the pullout device.

A new testing procedure, developed by Katz and Li [4], enables the preparation of specimens with high accuracy in fiber orientation and better control of the matrix around the fiber. Other test technique currently known (Wang et al. [5] and Larson et al. [6]), were found to be inadequate for obtaining the complete pullout behavior of micro-fibers, as they determine only the critical embedment length of the tested fiber. Thus a special pullout test technique had to be developed.

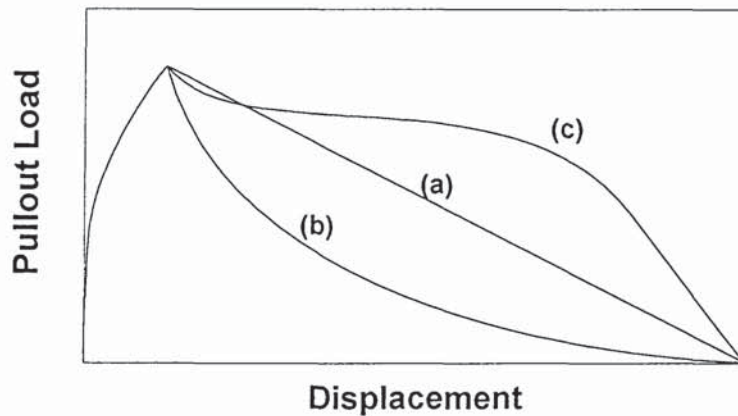


Fig. 1. Typical P-u curve based on friction (a), together with the effect of slip-weakening (b) and slip-hardening (c).

Table 1: Matrix composition

	Mix 1 0.35 LD	Mix 2 0.35 HD	Mix 3 0.5 LD	Mix 4 0.5 HD
Portland cement type III	200 gr	180 gr	200 gr	180 gr
Water	70 gr	46 gr	100 gr	76 gr
Silica-fume (slurry, 51% solids)	0 gr	41 gr	0 gr	41 gr
Superplasticizer	0 gr	4 gr	0 gr	2 gr
Water/binder	0.35	0.35	0.50	0.50
Silica-fume/binder	0	0.10	0	0.10

By using this procedure, a specimen with 5-15 fibers is prepared, as can be seen in Fig. 2a. The specimen is then sawn along the dashed line to provide a small specimen of a desired matrix thickness,  $L$  (Fig. 2b). Using a sensitive load-cell a pullout test is then performed, yielding the complete P-u curve of the fiber.

Bond strength was calculated according to equation 1, assuming a frictional bonding mechanism, and that the fiber fully debonds when the peak load  $P_{max}$  is achieved prior to slippage.

$$\tau = \frac{P_{max}}{\pi d L} \quad (\text{eq. 1})$$

where:  $P_{max}$  - maximum pullout load  
 $d$  - fiber diameter  
 $L$  - fiber embedded length

The fiber embedded length,  $L$ , was made as large as possible in order to allow a complete pullout of the fiber, without rupture. To improve the accuracy the actual fiber diameter was measured under the microscope for each individual fiber.

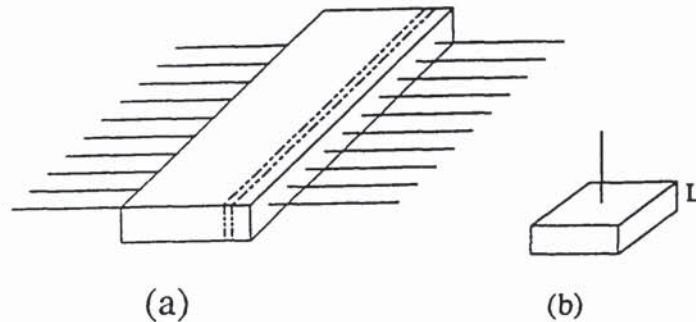


Fig. 2: Specimen after casting (a) and cutting (b)



## TEST RESULTS

### Pullout load - displacement curves

Typical pullout load-displacement curves of the various fibers are presented in Fig. 3. The dotted line in the figure represents the total embedded length of the fiber in the matrix.

The curves in Fig. 3 represent an average behavior of pullout of the fibers. Changes in the post peak behavior were observed for different matrices, as will be explained in the following:

- i) **Fiber A** - high modulus polyethylene (Fig. 3a). Slip-hardening was observed for all the matrices, with the slip-hardening becoming greater for the denser matrices.
- ii) **Fiber B** - steel (Fig. 3b). All fibers failed in tension prior to pullout. This was characteristic for all the matrices and even for short embedded length of 2-3 mm. The fracture load was also very low, much lower than the expected rupture load of such a fiber.
- iii) **Fiber C** - carbon, 10  $\mu\text{m}$  (Fig. 3c). The pullout load-displacement behavior of the fine carbon fiber was similar for the different matrices. For most cases, the decay of the load was linear, down to zero at complete pullout. For some cases of weak matrix, rapid decay was observed and the load was reduced down to zero slightly before complete pullout was achieved.

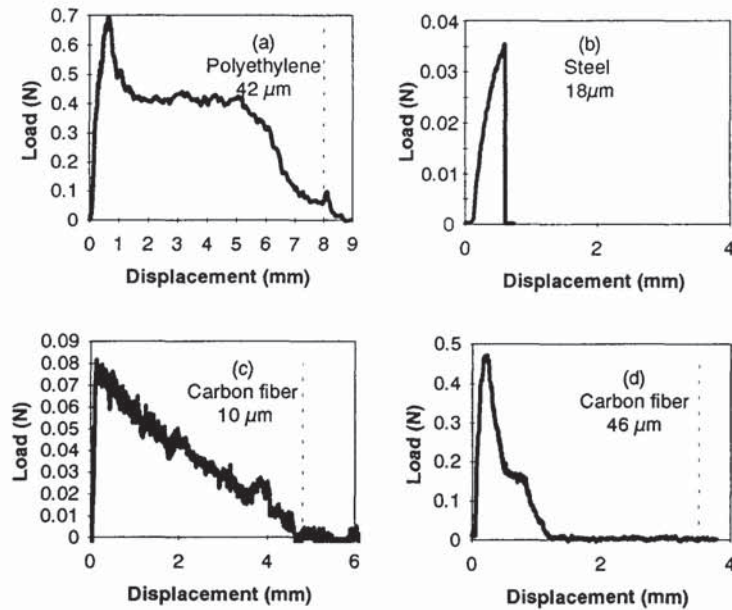


Fig. 3: Pullout load vs. displacement for: a. polyethylene fiber (Fiber A), b. steel fiber (Fiber B), c. thin carbon fiber (Fiber C), d. thick carbon fiber (Fiber D).

- iv) **Fiber D** - carbon, 46  $\mu\text{m}$  (Fig. 3d). The load decreased rapidly to zero after the maximum pullout load was achieved, much before complete pullout was reached. For the weak matrices, the decrease in load was moderated while more rapid decrease was observed for the denser matrices.

### **Bond Strength**

Bond strength results from the pullout tests are presented in Table 2 and Fig. 4. The numbers in parentheses in Table 2 are the coefficients of variation. Test results are based usually on 6 specimens, but in some instances, where large coefficients of variation were observed, up to 20 specimens were tested. For Fiber B (steel fiber), all fibers failed in tension, regardless of matrix composition. Therefore, its bond properties could not be determined. In addition, the special surface structure of Fiber B (as will be discussed later in the paper) prevented the measurement of the true cross-section area of the fiber. Thus, an estimation of a minimum value for the bond strength, basing on the maximum load achieved, could not be obtained.

The bond strength values of fibers A and C are quite similar to those measured by Li et al. [7] for high modulus polyethylene fiber, and estimated by Katz and Bentur [8] for thin carbon fibers, confirming the reliability of the new testing procedure.

**Table 2:** Results of bond strength from pullout test

	Fiber A (Polyethylene)	Fiber C (Carbon 10 $\mu\text{m}$ )	Fiber D (Carbon 46 $\mu\text{m}$ )
0.35 LD	0.56 MPa (28%)	0.80 MPa (14%)	0.39 MPa (73%)
0.35 HD	0.61 MPa (39%)	1.29 MPa (14%)	>3.02 MPa* (20%)
0.50 LD	0.40 MPa (19%)	0.52 MPa (31%)	0.52 MPa (49%)
0.50 HD	0.63 MPa (19%)	0.66 MPa (16%)	>2.44 MPa* (23%)

\* The results represent a minimum value only.

**Effect of w/b ratio:** Lowering the w/b ratio usually resulted in a better bond. The increase was greater for the small diameter carbon fibers. For this kind of fibers, lowering the w/b ratio from 0.5 to 0.35 resulted in an increase of 54% and 94% in the bond strength for matrices with no silica fume, and 10% silica fume, respectively. For the polyethylene fibers the changes were more moderate, and could not be identified clearly for the large diameter carbon fibers due to the high scattering of the results.

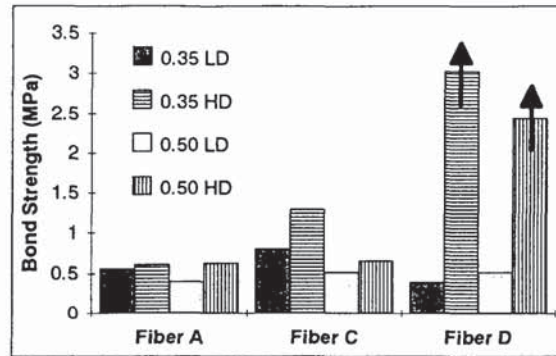


Fig. 4: Bond strength of fibers A, C and D for different matrices

**Effect of silica fume:** Introducing silica-fume into the matrix improved the bond strength of all the fibers. The strongest effect was on the bond strength of the thick carbon fibers (Fiber D) where an increase of 770% and 470% in the bond strength was observed for the low and high w/b ratio, respectively. When testing this type of fiber, embedded in matrices containing 10% of silica fume, many fibers broke in tension before pullout was achieved, and therefore the values presented in Table 2 are a minimum value only, calculated based on the results of the fibers which successfully pulled out and those which broke at the minimum embedded length.

#### Environmental Scanning Electron Microscopy (ESEM)

Typical ESEM photomicrographs of the fibers pulled from the cement matrix are presented in Figs. 5a through 5d for Fibers A to D, respectively. Fiber B looks more like a plexus of very fine filaments while the other fibers look like a solid single fiber. Special attention should be given to long grooves along the thick carbon fiber D. The grooves are relatively narrow ( $<4 \mu\text{m}$ ) and partially filled with hydration products, marked by the arrow in Fig. 4d. Unfortunately, good quality observation on the surface of Fiber A, at the part which was embedded in the matrix, could not be achieved due to curling of the fiber. However, squashing marks caused by rigid particles could be seen on the surface of this type of fiber.

#### DISCUSSION AND CONCLUSIONS

The results of the pullout tests and ESEM observations indicate a bond mechanism based on friction and mechanical anchorage, with changes in the interface as the pullout process proceeds, depending on the matrix composition.

Fiber A and Fiber C (high modulus polyethylene and small diameter carbon) are very smooth fibers (Figs. 5a and 5c). However, the carbon fiber is much harder than the polyethylene fiber. The mechanism of bond, for the two fibers, is more of mechanical friction, with more damage to

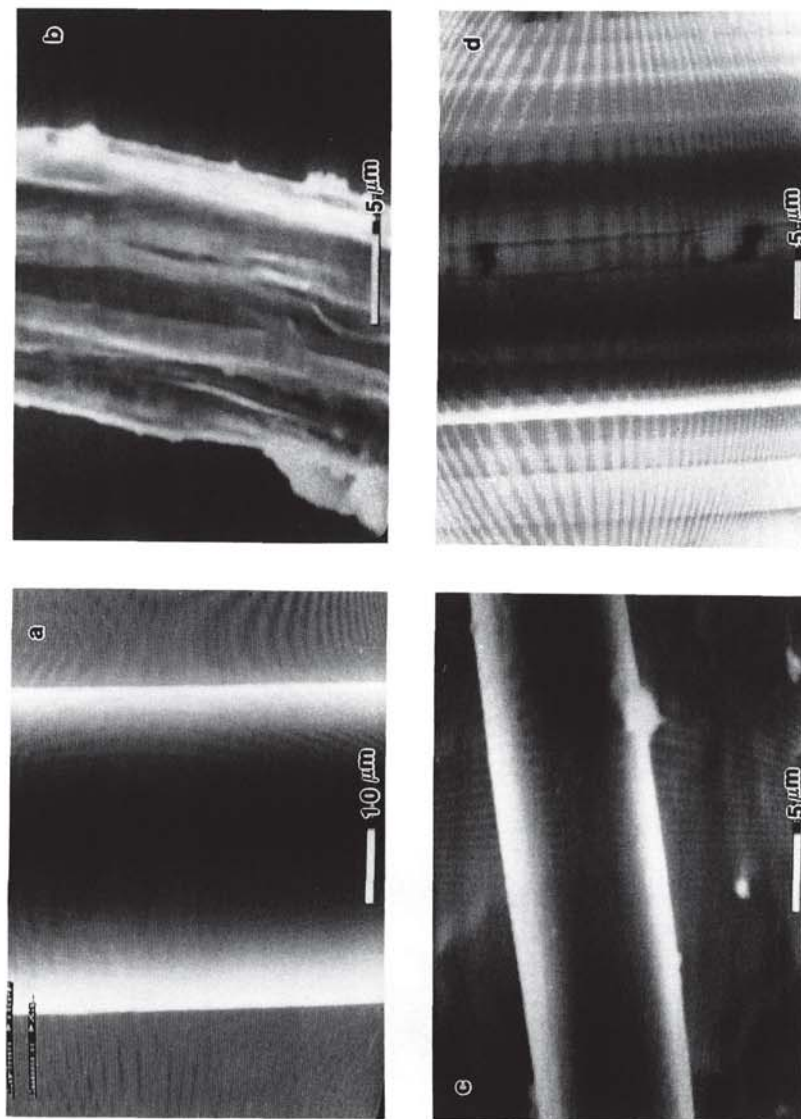


Fig. 5: ESEM photomicrograph of the surface of the fibers; (a) polyethylene (Fiber A), (b) steel (Fiber B), (c) carbon 10  $\mu\text{m}$  (Fiber C) and (d) carbon 46  $\mu\text{m}$  (Fiber D).



the polymeric fiber as the matrix becomes denser and stronger. Crumbs from the dense matrix trap at the fiber-matrix interface and squash into the fiber as it slips out, leading to a slip hardening behavior. The denser matrices (low w/b or matrices containing silica-fume) led to more damage to the fiber resulting in more pronounced slip-hardening behavior of this fiber.

Fiber C, which is denser than Fiber A, did not suffer from any damage to its surface. The linear decrease of the load after maximum pullout load is a characteristic of uniform friction mechanism of pullout.

Fibers B (steel) and D (thick carbon) show a characteristic behavior of a mechanical anchorage. It is possible that the structure of the steel fiber, which was made from a plexus of very fine filaments with an open structure (see Fig. 5b), allows the penetration of hydration products in-between the individual filaments resulting in good anchorage of the fiber in the matrix. This is probably the reason for the rupture of all the fibers of type B regardless of the cement matrix composition, and for the low loads needed for rupture.

For Fiber D, it seems that penetration of cement products into the long grooves observed on the fiber surface plays an important role in the mechanical connection between the fiber and matrix. Good penetration of the matrix into these grooves can provide a good mechanical anchoring between the fiber and the matrix. The drop of the pullout load after the peak, observed for this type of fiber, can be explained by breakage of the matrix penetrated into the grooves at the fiber surface, which leads to a severe reduction in the loads.

When using matrices of plain cement, with cement grain dimension comparable to or larger than groove width, the penetration of the matrix into the small grooves is poor, due to size effect and probably also due to the formation of a porous transition zone around the fiber, as shown for larger steel fibers (Bentur et al. [9], Wei et al. [10]) and aggregates (Goldman and Bentur [11]). This leads to poor and inhomogeneous mechanical bond, as can be seen in Table 2 by the low bond value and high coefficient of variation. In contrast, the use of ultra-fine particles such as silica fume (size  $<0.1 \mu\text{m}$ ) is expected to cause densification of the transition zone as well as good penetration into the grooves. These effects may explain the remarkable increase in bond strength when silica fume is used with Fiber D, described earlier.

#### **ACKNOWLEDGMENTS**

This research was partially funded by a grant to the ACE-MRL from Conoco Inc. which also manufactured Fiber D especially for this research.

#### **REFERENCES**

1. Li, V.C. ASCE Journal of Materials in Civil Engineering, **4**, (1), 41-57 (1992).
2. Wang, Y., Li, V.C. and Backer, S. The International Journal of Cement Composites and Lightweight Concrete, **10**, (3), 143-149 (1988).
3. Naaman, A.E. and Shah, S.P. Journal of the Structural Division, American Society of Civil Engineering, **102**, (ST8), 1537-1548 (1976).



4. Katz, A. and Li, V.C. Submitted for publication in the Journal of Materials Science Letters (1994).
5. Wang, Y., Backer, S. and Li, V.C. Journal of Materials Science Letters, **7**, 842-844 (1988).
6. Larson, B.K., Drzal, L.T. and Sorousian, P. Composites, **21** (3), 205-215 (1990).
7. Li, V.C., Wu, H.C. and Chan, Y.W. "Advanced Technology on Design and Fabrication of Composite Materials and Structures", Ed. Carpinteri and Sih (1993).
8. Katz, A. and Bentur. Accepted for publication in the Advanced Cement Base Materials Journal (1994).
9. Bentur, A., Diamond, S. and Mindess, S., Journal of Materials Science, **20**, 3610-3620 (1985).
10. Wei, S., Mandel, J.A. and Said, S. ACI Materials Journal, **83**, 597-605 (1986).
11. Goldman, A. and Bentur, B. Cement and Concrete Research, **23** (4), 962-972 (1993).